Gold Nanoparticles Immobilized on Stimuli Responsive Polymer Brushes as Nanosensors

Smrati Gupta,* Mukesh Agrawal, Petra Uhlmann, Frank Simon, Ulrich Oertel, and Manfred Stamm*

Leibniz-Institut für Polymerforschung Dresden e.V., Hohe Strasse 6, 01069 Dresden, Germany

Received July 10, 2008; Revised Manuscript Received August 21, 2008

ABSTRACT: We report on the immobilization of gold nanoparticles on end-functionalized and solvent responsive polystyrene brushes, grafted on an underlying substrate. The presence of gold nanoparticles on polystyrene brushes was confirmed by atomic force microscopy (AFM) and X-ray photoelectron spectroscopy (XPS). The resulting polystyrene−Au nanoassemblies have been used as the nanosensors for the detection of a variety of organic solvents in surrounding media. The sensing mechanism is based upon the change in the proximity of the immobilized gold nanoparticles as a consequence of the solvent induced reversible swelling−deswelling of polystyrene chains. The sensing ability was demonstrated by a simple analytic tool, i.e., UV−vis spectroscopy, through a shift in plasmon resonance band of immobilized Au nanoparticles. A dramatic blue shift of 32 nm in the surface resonance band was observed as the surrounding media of Au immobilized polystyrene brushes (Au−PS) was changed from air to the toluene. The described approach is facile and versatile in nature, which can be used for the fabrication of a variety of nanosensors based on the polymer brushes−nanoparticle assemblies.

Introduction

There has been an immense interest surrounding the synthesis, physical characterization, and manipulation of nanometer-scale particles in the past decade. Metal/metal oxide nanoparticles have been synthesized out of a variety of materials[1] in very well-defined sizes and with a variety of properties (e.g., metallic, conductive, semiconductive, insulating, or magnetic).[2−4] They have been potentially used in a wide spectrum of applications that range from optoelectronic devices[5] to biological sensors.[6] Recently, gold nanoparticles (Au NPs) have become increasingly important material for cutting-edge applications in fabrication of advanced optoelectronic devices by virtue of their tunable optical properties, which are strongly dependent on the particle size and shape, interparticle distance, nature of the protecting organic shell, and surrounding media. They are very sensitive to change in optical parameters in their surroundings. Exploitation of this unusual phenomenon has given rise to new analytical and sensing techniques. The colloidal dispersions of Au nanoparticles exhibit particular colors due to collective oscillations of electrons in the vicinity of the surface by visible light and show a colorimetric response to a change in the interparticle distance.[7] For example, Nath et al.[8] reported the fabrication of a biosensor made of Au NPs deposited on a glass substrate. Mirkin and co-workers[9] have used DNA-tethered colloidal Au particles to develop an optical method for detection of DNA hybridization. Tokareva et al.[10] reported fabrication of nanosensor based on the change in surface plasmon resonance of Au NPs with change in pH of surrounding water. In addition, Emory and Nie[11] have studied surface-enhanced Raman scattering (SERS) from single, surface-confined gold and silver (Ag) nanoparticles. Similarly, the heightened interparticle electric field[12] in deliberately prepared metal nanoparticle−analyte−metal nanoparticle sandwiches has been used to generate strong SERS signals from the sandwiched analyte.[13] Electrochemical sensors for peroxide and other small molecules have been developed using surface confined protein/Au colloid complexes.[14]

In all these examples, potential applications required positioning of nanoparticles in complex two- and even three-dimensional structures. A crucial issue is the positional stability of particles on a surface, or in a structure, after they have been deposited. A number of protocols ranging from self-assembly to nanomanipulation with a scanning probe microscope (SPM) have been proposed to achieve this goal.[15] Among all, two approaches have been most commonly used for particle stabilization. One involves the use of self-assembled monolayers (SAMs) to surround the nanoparticles. SAMs have attracted considerable interest during the past two decades and are formed spontaneously by immersing substrates in dilute solutions of amphiphilic molecules in appropriate solvents.[16] A variety of film/ substrate systems are known to lead to the formation of these highly ordered monolayer films.[17] The alternative approach involves exploitation of polymer chains, tethered by one end to the underlying substrate in brush conformation. This methodology has a number of advantages over the conventional methods of the nanoparticles' stabilization on macroscopic surfaces. For example, (1) polymer brushes can be grown on a variety of functional surfaces exploiting "grafting to" or "grafting from" approaches, (2) grafted polymer chains can withstand harsh operational conditions of solvent and temperature, and (3) length and grafting density (number of chains per unit area of grafted surface) of the polymer brushes can be manipulated in a wide range via selecting the polymer chains of suitable molecular weight (MW). The grafting density determines the conformation of polymer chains, which in turn governs the effectiveness of polymer coating for a given application, and (4) above all, polymer brushes are capable of responding to changes of temperature, solvent polarity, pH, and other stimuli, generally by reversible swelling/deswelling, which lead to the changes in optical properties of adsorbed nanoparticles and open a new avenue for nanosensors. Only very few studies have been reported in the literature on immobilization of nanoparticles using this approach.[10,18] Tokareva et al.[10] reported the fabrication of novel nanosensors based on the variation in distance between the Au NPs adsorbed on poly(2-vinylpyridine) polymer brushes and those deposited on the substrate, with the change in pH of surrounding media. Similarly, Mitsuishi et al.[18c] demonstrated temperature induced change in optical properties of gold nanoparticles, assembled on substrate with temperature responsive PNIPAM (poly-*N*-isopropylacrylamide) brushes.

* To whom correspondence should be addressed. E-mail: gupta@ipfdd.de; stamm@ipfdd.de.

10.1021/ma801557u CCC: $40.75
Published on Web 10/15/2008

Scheme 1. Schematic Representation of Solvent Induced Reversible Swelling of Au−PS Brushes

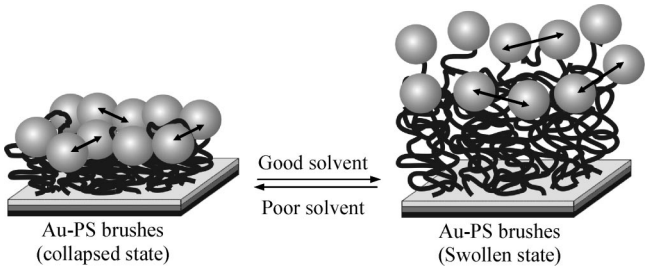

Recently, we reported on the immobilization of Ag nanoparticles on pH responsive poly(2-vinylpyridine) brushes and demonstrated application of resulting P2VP−Ag nanoassemblies in the fabrication of pH nanosensors.[19] Extending the applicability of this approach, we report on the fabrication of nanosensors which can sense the presence of organic solvents in surrounding media based on the solvent induced swelling and deswelling of polymer brushes coupled with optical changes in localized surface plasmon resonance (LSPR) of Au NPs. The process involves immobilization of Au nanoparticles on the silicon surface using responsive ultrathin polystyrene brushes. The physical interaction (hydrogen bonding) between hydroxyl groups of end functionalized, chemically grafted polystyrene chains and carboxylic groups of surface functionalized Au nanoparticles is the driving force of the fabrication of these hybrid nanoassemblies. The sensing approach has been demonstrated by the observed shift in the absorption maximum of Au nanoparticles, provoked by the change in organic solvents in surrounding media of polymer brushes, as shown in Scheme 1.

Experimental Section

Materials. α-Hydroxy-ω-carboxy-terminated polystyrene (M_n = 9500 g mol^{-1}) and polyglycidyl methacrylate (M_n = 17 500 g mol^{-1}) was purchased from Polymer Source, Inc., and used as received. Hydrogen tetrachloroaurate(III) ($HAuCl_4 \cdot 4H_2O$), tetraoctylammonium bromide (TOAB), 11-mercaptoundecanoic acid (MUA), and sodium borohydride ($NaBH_4$) all were purchased from Aldrich and used without additional purification. Highly polished single-crystal silicon wafers of {100} orientation with ca. 1.5 nm thick native silicon oxide layers were purchased from Semiconductor Processing Co. and used as substrates. Acetone, ethanol, dichloromethane (DCM), chloroform ($CHCl_3$), cyclohexane, toluene, and tetrahydrofuran (THF) were dried using standard methods before use.

Instrumentation. Transmission electron microscopy (TEM) images of Au nanoparticles were recorded on Zeiss Omega 912 microscope at an accelerating voltage of 200 kV. Samples were prepared via drying a drop of toluene dispersion on a carbon-coated copper grid. IR spectra of functionalized Au nanoparticles were recorded with a Mattson Instruments Research Series 1 FTIR spectrometer. Prior to analysis, dried samples were mixed with KBr pellets. The thickness of polymer layers in the dry state was measured at $\lambda = 632.8$ nm and an angle of incidence of 70° with a null ellipsometer in a polarizer compensator−sample analyzer (Multiscope, Optrel Berlin) as described elsewhere.[20] From the obtained values, we calculated the distance between grafting points by the following equation:

$$d_g = \sqrt{\frac{M_n}{H\rho N_A}} \tag{1}$$

where H is the ellipsometric thickness, ρ is the mass density (1.04 g/cm^3), N_A is Avogadro's number, and M_n is the molecular weight. "In situ" ellipsometric measurements were performed in a quartz cuvette (Hellma, Müllheim, Germany) to examine the swelling behavior of the polymer brushes in different solvents. The measurements were performed for each sample after each step of the modification to use the measurements of the previous step as a reference for the simulation of ellipsometric data.[20] The refractive indices used for the calculations were 3.858-i0.018, 1.4598, 1.525, and 1.59 for silicon substrate, native silica layer, PGMA layer, and PS brushes, respectively. XPS experiments were performed with an AXISULTRA spectrometer (Kratos Analytical, U.K.) equipped with a monochromized Al Kα X-ray source of 300 W at 20 mA. The survey spectra and high-resolution spectra were obtained at analyzer's pass energy set value of 160 and 20 eV, respectively. All spectra were charge compensated using the C_xH_y component peak of the C 1s spectra at BE (binding energy) 285.00 eV as reference peak.[21] To determine elemental ratios, normalized peak areas (ϕ) were calculated from peak areas (A) of survey spectra, respecting experimentally determined sensitivity factors and the spectrometer's transmission function using the following equation:

$$\phi = \frac{A}{\mathrm{RSF}\cdot\mathrm{Tx}} \tag{2}$$

where RSF is the respecting sensitivity factor[22] and Tx is the spectrometer's transmission function. The advancing water contact angle was measured using "DSA-10" Krüss equipment with an accuracy of 0.5°. For UV−vis measurements, samples were prepared on a glass substrate, which has been cleaned using the same procedure as employed for silicon substrates. Samples were put in a cleaned quartz cuvette and then filled with the respective solvent. In a reference cuvette, a cleaned and bare glass substrate (without brushes and NPs) was taken and filled with the same solvent. Immediately (after ∼40−60 s), samples were irradiated with UV light and spectra were recorded with a Cary 50 spectrophotometer (Varian). Atomic force microscopy (AFM) studies were performed with a Dimension 3100 (Digital Instruments, Inc., Santa Barbara, CA) microscope. Tapping mode was used to map the film morphology at ambient conditions. We estimated the surface coverage of immobilized nanocrystals by the following equation:

$$\varphi = \frac{100\% N\pi d^2}{4A} \tag{3}$$

where d is the diameter of the nanocrystals and N is the number of nanocrystals detected per area A.

Preparation of Polymer Brushes. Polystyrene brushes were grown on silicon substrates by the "grafting to" method as described elsewhere.[23] Silicon wafers (2 cm × 1 cm) were cleaned with dichloromethane in an ultrasonic bath for 30 min, placed in 1:1 mixture of 29% ammonium hydroxide and 30% hydrogen peroxide (*warning: this solution is extremely corrosive and should not be stored in tightly sealed containers due to evolution of gas*) for 1.5 h, and rinsed several times with Millipore water. A thin layer of PGMA (ca. 2 nm) was deposited on substrate by spin-coating from a 0.02% w/w solution in chloroform and annealed at 110 °C for 10 min. Subsequently, a thin film of α-hydroxy-ω-carboxy-terminated polystyrene (2% w/w solution in toluene) was spin-coated and annealed at 150 °C for 3 h. Ungrafted polymer was removed using Soxhlet extraction in toluene for 4 h.

Preparation of Gold Nanoparticles. Gold nanoparticles were synthesized by borohydride reduction of chlorauric acid as described elsewhere with some modifications.[24] In a typical process, 328 mg of TOAB (0.6 mmol) dissolved in 100 mL of toluene was mixed with 50 mL of an aqueous solution of $HAuCl_4 \cdot 4H_2O$ (15 mM) at room temperature. Subsequently, a solution of 32.75 mg of MUA (0.15 mmol) in 25 mL of toluene was dropwise added into the reaction mixture and allowed to stir for 10 min under vigorous stirring. Thereafter, a freshly prepared 25 mL aqueous solution of 0.30 M $NaBH_4$ was added, and resulting mixture was stirred for 1 h. The organic phase was separated and well-washed with distilled

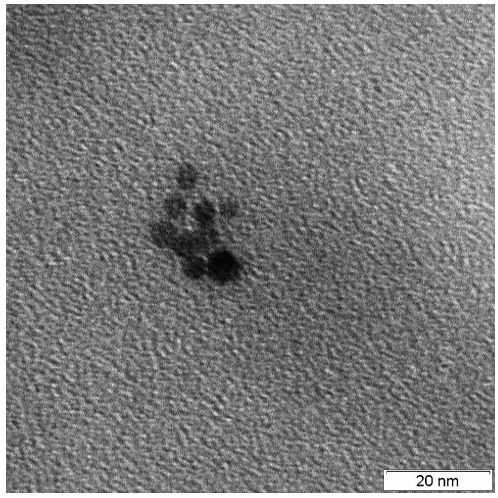

Figure 1. TEM image of Au nanoparticles.

water followed by the drying under reduced pressure. The resulting black solid was heat treated at 155 °C at the heating rate of 2 °C min^{-1} for 30 min. The heat-treated product was dissolved in 10 mL of toluene, mixed with 200 mL of chloroform to remove the excess TOAB and MUA, and finally resulting Au NPs were separated from reaction media through centrifugation.

Immobilization of Gold Nanoparticles on PS Brushes. Au nanoparticles were attached on the PS polymer brushes from a 1 mM solution in toluene by incubating the samples overnight. Nonadsorbed or weakly adsorbed particles were removed by several times rinsing with toluene.

Results

Well-defined and homogenously distributed end functionalized PS brushes were prepared on a silicon substrate exploiting the well-known "grafting to" approach.[23] The process involves chemisorption of PGMA anchoring layer on silicon substrate followed by the chemical grafting of bifunctionalized PS polymer chains. A thin layer of PGMA (as an anchoring layer) was deposited on cleaned silicon wafer. It has been investigated earlier that PGMA can serve as a universal anchor for different types of polymer brushes on wide range of substrates including silicon, glass, alumina, gold, and silver by virtue of the high reactivity of its epoxy groups toward hydroxyl groups of these surfaces.[25] The thickness of PGMA layer was found to be 2 ± 0.2 nm by ellipsometry. Bifunctionalized PS polymer chains were spin-coated on the PGMA layer, and samples were annealed at 150 °C for 3 h. It leads to the chemical grafting of PS chains on silicon substrate through the −COOH-terminated ends and offers −OH-terminated ends free for immobilization of Au nanoparticles. The presence of free −OH-terminated ends of grafted polystyrene brushes on the surface of silicon substrate was confirmed by XPS (see Figure 1 of the Supporting Information). Chemical reaction between −COOH groups of PS chains and epoxy units located in the "loops" and "tails" sections of the attached PGMA macromolecules leads to the chemical attachment of PS chains on Si wafer. Ungrafted polymer was removed by Soxhlet extraction in toluene for 4 h and thickness of washed and dried PS brushes was measured as 6.0 nm by ellipsometry. The advancing contact angle of obtained PS brushes was found around 83 ± 1.5° owing to the hydrophobic nature of polymer chains. Distance between the grafting points was estimated by eq 1 as 2.58 nm, which yielded the grafting density of obtained PS brushes as 0.15 nm^{-2}.

As shown in Figure 1, the TEM image confirmed the formation of Au nanoparticles with a mean size of 5.2 nm. The surface of the Au nanoparticles was chemically protected with a polar and lipophilic group, 11-mercaptoundecanoic acid, exploiting the affinity of Au for the thiol compounds.[26]

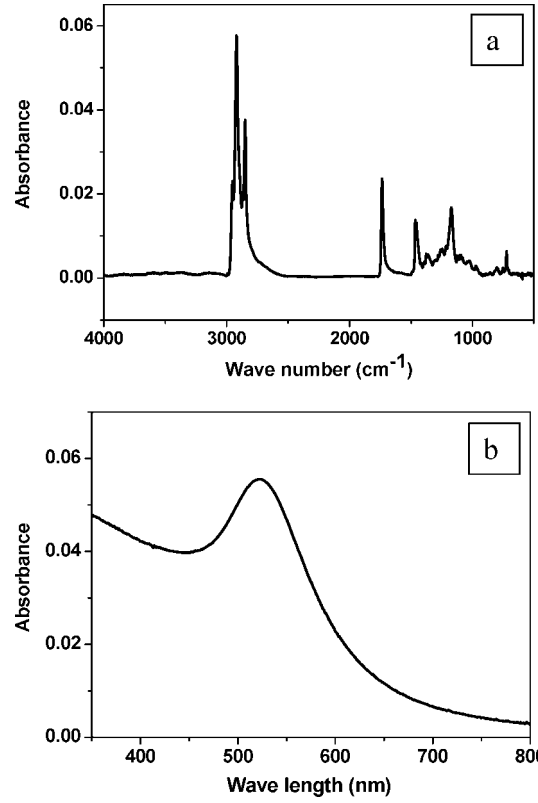

Figure 2. (a) IR spectrum and (b) UV−vis spectrum of 11-mercaptoundecanoic acid capped Au nanoparticles.

The presence of −COOH on the surface of nanoparticles was further confirmed by FTIR spectroscopy. Figure 2a shows a C═O stretching band at 1740 cm^{-1}, characteristic of free carboxylic acid groups.[27] In addition, the absence of the S−H peak at 2550 cm^{-1} confirms the attachment of this capping agent on the surface of gold nanoparticles through the thiol group.

Functionalization of Au nanoparticles with 11-mercaptoundecanoic acid not only provides the −COOH moiety to the Au nanoparticles to interact with the −OH groups of polystyrene chains but also enables them good solubility in toluene, which is a good solvent for polystyrene brushes. Here good solvent means to a solvent in which polymer brushes are well stretched due to a good interaction between polymer chain segments and solvent. Owing to the osmotic and entropic effects and van der Waals interactions between PS and solvent, all the polystyrene chains remain highly stretched in toluene. Simulations studies on polymer brushes have also revealed that chain ends are enriched in the top brush layer depending on chain stretching and grafting density.[28] As a consequence of that, Au nanoparticles present in the solution have access to most of the end functionalities of highly stretched polymer chains facilitating the immobilization process. Figure 2b shows UV−vis spectra of Au nanoparticles dispersed in toluene, indicating a strong characteristic absorption peak at 520 nm.

The immobilization of Au nanoparticles on polystyrene brushes was achieved by exploiting the physical interaction (hydrogen bonding) between free end functionality of grafted polystyrene chains (−OH groups) and surface functionality (−COOH groups) of Au nanoparticles. Overnight incubation of polystyrene brushes into the Au−toluene solution resulted in self-assembly of Au nanoparticles on the polymer brushes. Figure 3 illustrates AFM phase images of polymer brushes (a) before and (b) after the immobilization of Au nanoparticles.

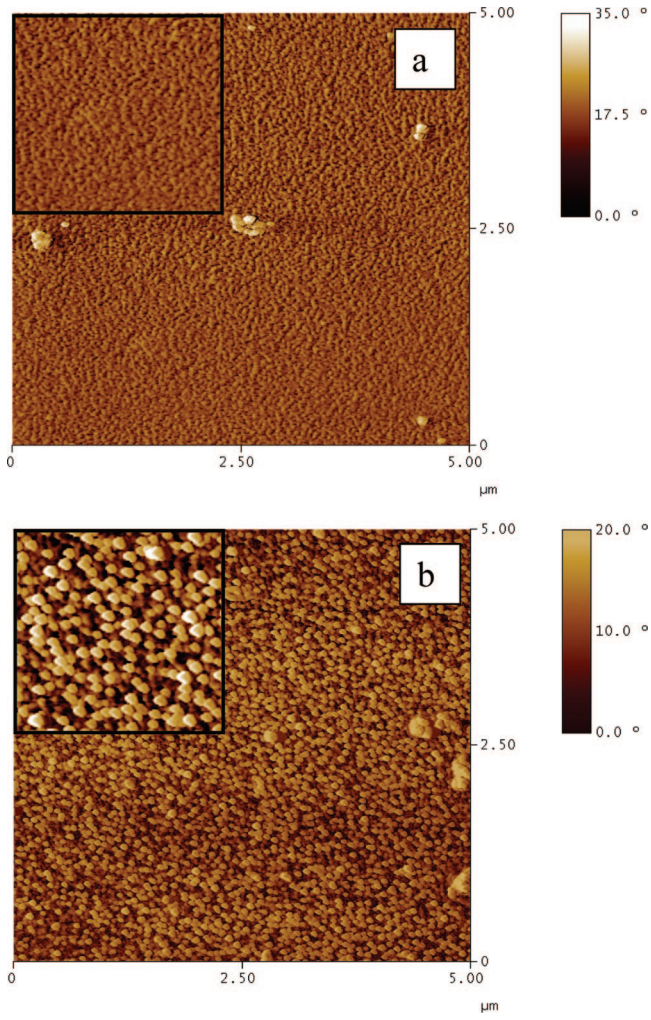

Figure 3. AFM images of polystyrene brushes (5 × 5 μm) (a) before and (b) after the immobilization of Au nanoparticles. Insets show enlarged views (1 × 1 μm) of a part of images.

These results indicate that immobilized Au nanoparticles formed a nearly uniform coverage on the polymer brushes. The root-mean-square (rms) roughness of the bare polymer brushes was measured ≤0.4 nm, which increased significantly to the 3.3 nm after the immobilization of Au nanoparticles. Moreover, a close inspection of these images reveals that sample has developed a "pebbled" appearance after the immobilization process, indicative of the presence of a layer of the nanoparticles on polystyrene brushes. In addition, these results coupled with eq 3 revealed that Au nanoparticles cover ~15% of brush surface area. The number of nanoparticles per area of the sample was counted by zooming a part of the AFM image. However, immobilized Au nanoparticles appear larger in AFM image than those shown in TEM image of Au NPs. This can be attributed to the AFM tip surface convolution effects.[29] The presence of the nonaggregated Au nanoparticle on polystyrene brushes was confirmed by the absence of the optical signature, i.e., an absorption at wavelengths greater than 600 nm, of the aggregate formation of Au nanoparticles in the UV−vis absorption spectrum of samples (as shown in Figure 5a).[30]

The presence of Au nanoparticles on polystyrene brushes was further proved by X-ray photoelectron spectroscopy (XPS) analysis. It should be noted that samples were repetitively washed with toluene before carrying out the measurements in order to ensure the complete removal of nonimmobilized Au nanoparticles. Figure 4 shows the XPS wide scan spectrum of the polystyrene brushes after the immobilization of Au nanoparticles (Au−PS brushes). In comparison to the wide scan spectrum of bare polystyrene brushes (shown in Figure 1 of the Supporting Information), the appearance of Au signals at the characteristic binding energies indicates the presence of Au nanoparticles on polymer brushes.[31]

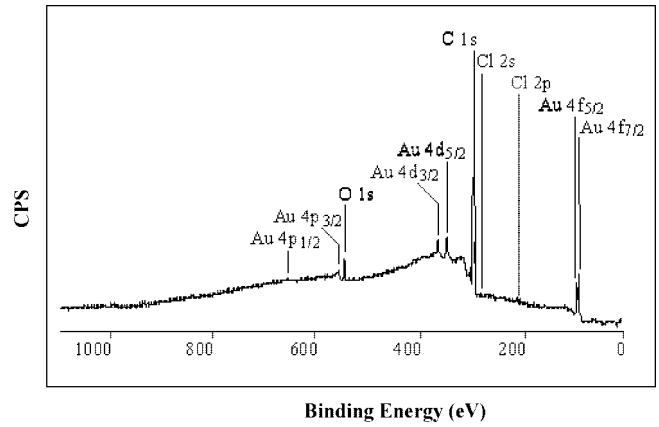

Figure 4. XPS survey spectrum (takeoff angle 75°) of polystyrene brushes after the immobilization of Au nanoparticles.

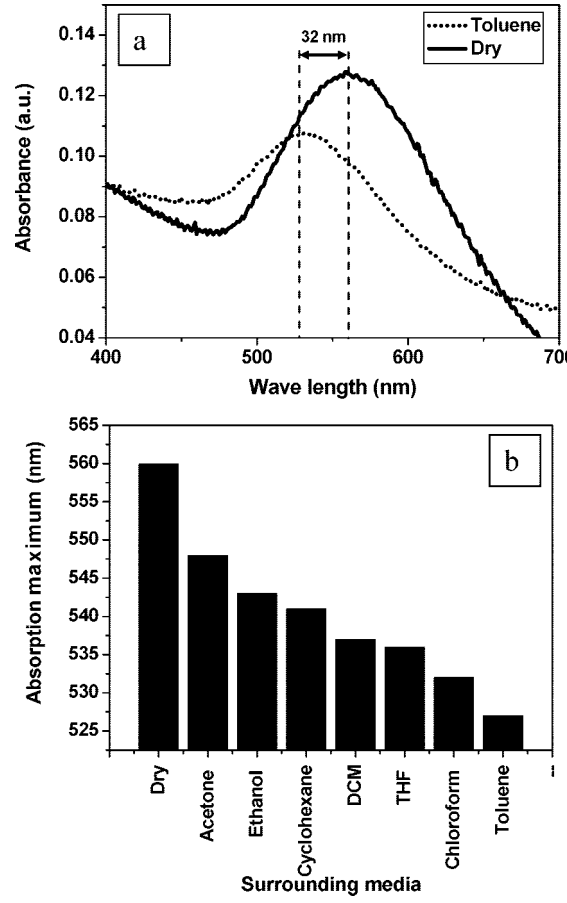

Figure 5. (a) UV−vis spectra of Au−PS brushes in dry and swollen (in toluene) states, (b) position of the absorption maxima of Au−PS brushes in different organic solvents.

Moreover, in order to prove that immobilized Au nanoparticles are located on the top of polymer brushes, we carried out XPS investigations of the samples at three different takeoff angles (angle between surface normal and electron-optical axis of the spectrometer), namely 0°, 60°, and 75°, which enabled to collect the information from different mean depths of 8, 4, and 2 nm, respectively, of the polymer brush layer.[32,33] These data indicate that the [Au]:[C] ratio gradually increases from

0.009 to 0.016 with increasing the takeoff angle, suggesting that most of the Au NPs are located at the top of brush layer. However, the appearance of Au signals even at 0° takeoff angle may be attributed to the dry state of the sample, employed for analysis. It is reasonable to assume that in dry state polymer chains are collapsed, and hence a fraction of the Au nanoparticles immobilized at the end of these polymer chains may be present inside the brush layer as well.

It has been realized that polymer chains, tethered to the substrates by one end in brush conformation, can show a solvent induced swelling/deswelling behavior.[34] On the basis of the nature of interaction with the grafted polymer chains, solvents can broadly be classified as poor and good solvents for a polymer brush. Polymer chains always remain in collapsed state in a poor solvents due to the poor interaction between solvent and polymer segments. On the contrary, they have a stretched conformation with increased mobility of their free ends in good solvents on account of good interaction between solvent and polymer segments. The thickness of the swollen layer is governed by the balance between osmotic pressure and chain stretching. Various studies employing analytical theory,[35] simulation,[36] and neutron reflection[37] have shown that stretched polymer chains in a polymer brush gradually shrink and finally collapse as the solvent quality changes from good to poor. We designed our sensing material exploiting this stimuli responsive property of polystyrene brushes. The proximity of the immobilized Au nanoparticles will be altered by swelling of their support polymer in response to the organic solvents. One can expect an increase in interparticle distance on swelling of the polymer brushes and a decrease in the same manner when brushes are collapsed. The change in proximity of immobilized Au nanoparticles could induce a shift in their plasmon absorption band. Recently, Kumacheva et al.[38] also demonstrated the solvent induced change in the position of plasmon resonance band of Au nanorods, coated with a bilayer of cetyltrimethylammonium bromide (CTAB) and end terminated with the polystyrene chains. They found that change in surrounding media from DMF to water−DMF mixture led to the variation in assembly of Au nanorods from side-by-side to the end-to-end one. With the addition of water, the mixture became poor solvent for the polystyrene chains but remained a good solvent for the hydrophilic CTAB layers. Moreover, a continuous increase in molecular weight of the polystyrene chains caused the Au nanorods to assemble in bundles and then nanochains. These solvent and molecular weight induced change in supraassembly of the nanorods enabled the manipulation in optical properties of Au nanorods. To observe the clear shift in surface plasmon resonance, the size and proximity of the Au nanoparticles immobilized on the polymer brushes are the critical factors. It has been reported that the appropriate size of the Au nanoparticles for this purpose is <20 nm in diameter.[39] Also, a narrow size distribution of the immobilized nanoparticles would be required for acquiring a sharp optical response.

Therefore, preparation conditions for Au nanoparticles and their concentration in absorption media were carefully selected.[40] When samples were immersed into toluene which is considered as a good solvent for polystyrene,[41,42] the thickness of polymer brushes was found to increase from 6 to 14.7 nm by ellipsometry (see Figure 2 of the Supporting Information). When the same sample was removed from the toluene, dried, and immersed into other solvents such as chloroform and ethanol, thickness as found to be changed to 11.6 and 6.3 nm, respectively, suggesting the presence of a less stretched and collapsed conformation of polymer chains in these solvents. In accordance with the literature,[41] the degree of the swelling or conformation of polymer chains in different organic solvents and hence organization of immobilized Au nanoparticles were found to be governed by the quality of the solvent.

The UV−vis measurements conducted in various organic solvents elucidated the sensitivity and dynamic range of the optical response of nanohybrid assemblies. Figure 5a shows that the plasmon absorption band originally appeared with a maximum absorbance at 560 nm when brushes are in dry state. When polymer brushes were immersed in toluene, the absorption band was found to appear at 528 nm, showing the dramatic blue shift of 32 nm with respect to that of gold nanoparticles on dry polymer brushes. It can be attributed to the solvent induced swelling of polymer chains and higher mobility of their free ends in toluene, which caused increase in interparticle distance of Au nanoparticles, located at the top of polymer chains (as shown in Scheme 1). Furthermore, when surrounding media was changed from toluene to ethanol, the absorption maxima was found to shift from 528 to 543 nm as ethanol is a poor solvent for polystyrene and brushes are expected to be collapsed in this surrounding medium. It is worth mentioning that this solvent induced shift in absorption maxima of immobilized Au nanoparticles was found to be completely reversible. Variation in the position of plasmon absorption band with different organic solvents is depicted in Figure 5b. The UV−vis spectra of Au−PS brushes in these solvents are shown in Figure 3 of the Supporting Information. A closer inspection of UV−vis spectra taken in various organic solvents reveals a weak shoulder at the 560 nm, which can be attributed to the slight aggregation of immobilized Au NPs even after immersing the sample in the respective solvent. These results reveal that absorption band positions are controlled by the nature of the organic solvents.[41]

Recently, Tokareva et al.[10] reported the fabrication of pH nanosensors and demonstrated the shift in surface resonance band by manipulating the distance between the Au nanoparticles adsorbed on poly(2-vinylpyridine) brushes and those deposited on the substrate by causing the pH induced swelling of P2VP chains. In comparison to this study, the sensing mechanism of our nanoassemblies is based on the change in interparticle distance of Au nanoparticles located on the top of polymer chains. Moreover, the employed polymer support, i.e. polystyrene brushes, is responsive to a series of organic solvents as shown in Figure 5b. It is also important to emphasize here that this shift in absorption maxima is not induced by the change in refractive index of surrounding solvent. If it were so, we would have observed only a red shift in the maximum position with increase in refractive index of solvent, as reported by Nath et al.[43] In contrast, we observed that the absorption band position depends on the solvent quality irrespective of their refractive index. It strongly suggests that solvent induced change in conformation of chemically grafted polystyrene chains is the driving force for this modulation of the position of plasmon resonance band.

Discussion

We demonstrated the fabrication of an extremely straightforward but highly sensitive nanosensor, based on solvent induced swelling of polystyrene brushes coupled with surface plasmon resonance of immobilized Au nanoparticles. The resulting PS−Au nanoassemblies have been exploited in the fabrication of solvent nanosensors. In addition, the described methodology demonstrates an effective way to the homogeneous and tailored organization of nanoparticles on macroscopic surfaces. In comparison to the previously reported studies on the polymer brushes−nanoparticles assemblies, the described system has the following advantages: (1) Unlike the P2VP−CdSe system reported by Ionov et al.,[18b] the presented system has a wide applicability allowing to detect a series of the organic

solvents in surrounding media (as shown in Figure 5b) rather than only ethanol and toluene. In addition, we believe that it should work at lower pH also as Au nanoparticles are quite stable at wide range[10] of pH unlike the CdSe nanoparticles. (2) The described approach exploits an extremely simple analytical setup (UV−vis spectroscopy) to detect the variation in optical properties of the system as compared to those used in previously reported studies.[10,18b] (3) A well-planned synthetic strategy allowed us to immobilize the Au nanoparticles selectively at the end of polystyrene chains rather than randomly on polymer brushes as reported for other systems.[10,18b] We believe this feature allowed us to get a large shift in surface plasmon band position of Au nanoparticles from collapsed conformation to the stretched confirmation of polystyrene chains. (4) In addition, the hydrogen bonding between surface functionality −COOH of immobilized nanoparticles and free end functionality −OH of polymer chains offers a relatively strong adhesion between these two components rather than hydrophobic−hydrophobic interaction claimed by Ionov et al.[18b] for the P2VP−CdSe system. However, we admit that this interaction is not as much strong as between Ag NPs and polymer brushes, reported in our previous study.[19] (5) In a marked difference with previously reported systems,[10,18b] our system is not limited to the reflective surfaces as it is based only on change in interparticle distance of absorbed particles caused by swelling/deswelling of polystyrene brushes irrespective of the nature of substrate in terms of roughness and reflectivity. (6) In addition, if we think only in the context of the immobilization of nanoparticles on planar substrates, the brush conformation of surface modifier such as polystyrene brushes in present case renders much more binding sites as compared to a thin layer of polymer as reported by Malynych et al.[44] In addition, it offers a selective and homogeneous distribution of nanoparticles on macroscopic surfaces. As evident by UV−vis spectra of Au immobilized polymer brushes, no optical signature for aggregation of the nanoparticles has been observed, indicating that employed approach is more efficient to achieve the immobilization of nanoparticles with homogeneous distribution. (7) Above all, this approach is versatile in nature as can be used for the fabrication of nanosensor devices based on temperature, pH, and ionic strength responsive polymer brushes.

Acknowledgment. The authors gratefully acknowledge the help of Mrs. Gudrun Adam and Mr. Alex Menze in IR and TEM analysis of samples, respectively.

Supporting Information Available: Wide scan XPS spectrum of bare PS brushes, ellipsometric thickness of PS brushes in toluene, and UV−vis spectra of Au immobilized PS brushes in different solvents. This material is available free of charge via the Internet at http://pubs.acs.org.

References and Notes

(1) (a) Handley D. A. *Colloidal Gold: Principles, Methods, and Applications*; Hayat, M. A., Ed.; Academic Press: San Diego, 1989.
(2) (b) Gorer, S.; Hsiao, G. S.; erson, M. G.; Stiger, R. M.; Lee, J.; Penner, R. M. *Electrochim. Acta* **1998**, *43*, 2799. Collier, C. P.; Vossmeyer, T.; Heath, J. R. *Annu. Rev. Phys. Chem.* **1998**, *49*, 371, and references therein.
(3) Ni, Y. H.; Ge, X. W.; Xu, X. L.; Chen, J. F.; Zhang, Z. C. *J. Inorg. Mater.* **2000**, *15*, 9.
(4) Gangopadhyay, R.; De, A. *Chem. Mater.* **2000**, *1*, 608, and references therein.
(5) Sato, R.; Ahmed, H.; Brown, D.; Johnson, B. F. G. *J. Appl. Phys.* **1997**, *82*, 696.
(6) Elghanian, R.; Storhoff, J. J.; Mucic, R. C.; Letsinger, R. L.; Mirkin, C. A. *Science* **1997**, *277*, 1078.
(7) (a) Takeuchi, Y.; Ida, T.; Kimura, K. *Surf. Rev. Lett.* **1996**, *3*, 1205–1208. (b) Kreibig, U.; Genzel, L. *Surf. Sci.* **1985**, *156*, 678–700.
(8) Nath, N.; Chilkoti, A. *Anal. Chem.* **2004**, *76*, 5370–5378.
(9) (a) Mirkin, C. A.; Letsinger, R. L.; Mucic, R. C.; Storhoff, J. J. *Nature (London)* **1996**, *382*, 607. (b) Elghanian, R.; Storhoff, J. J.; Mucic, R. C.; Letsinger, R. L.; Mirkin, C. A. *Science* **1997**, *277*, 1078. (c) Storhoff, J. J.; Elghanian, R.; Mucic, R. C.; Mirkin, C. A.; Letsinger, R. L. *J. Am. Chem. Soc.* **1998**, *120*, 1959.
(10) Tokareva, I.; Minko, S.; Fendler, J. H.; Hutter, E. *J. Am. Chem. Soc.* **2004**, *126*, 15950–15951.
(11) Nie, S.; Emory, S. R. *Science* **1997**, *275*, 1102–1106.
(12) (a) Sestak, O.; Matejka, P.; Vlckova, B. *Collect. Czech. Chem. Commun.* **1996**, *61*, 59. (b) Keating, C. D.; Kovaleski, K. K.; Natan, M. J. *J. Phys. Chem. B* **1998**, *102*, 9414–9425.
(13) Brandt, E. S.; Cotton, T. M. Surface-enhanced Raman Scattering. In *Investigations of Surfaces and Interfaces Part B*; Rossiter, B. W., Ed.; John Wiley & Sons: New York, 1993; Vol. *IXB*, p 633.
(14) (a) Zhao, J.; Henkens, R. W.; Stonehuerner, J.; O'Daly, J. P.; Crumbliss, A. L. *J. Electroanal. Chem.* **1992**, *327*, 109. (b) Henkens, R. W.; Kitchel, B. S.; O'Daly, J. P.; Perine, S. C.; Crumbliss, A. L. *Recl. Trav. Chim. Pays-Bas* **1987**, *106*, 298.
(15) (a) Ohara, P. C.; Heath, J. R.; Gelbart, W. M. *Angew. Chem., Int. Ed. Engl.* **1997**, *36*, 1077. (b) Perkins, F. K.; Dobisz, E. A.; Brandow, S. L.; Calvert, J. M.; Kosakowski, J. E.; Marrian, C. R. K. *Appl. Phys. Lett.* **1996**, *68*, 550. (c) Bandyopadhyay, S.; Miller, A. E.; Chang, H. C.; Banerjee, G.; Yuzhakov, V.; Yue, D.-F.; Ricker, R. E.; Jones, S.; Eastman, J. A.; Baugher, E.; Chandrasekhar, M. *Nanotechnology* **1997**, *7*, 360. (d) Mirkin, C. A.; Letsinger, R. L.; Mucic, R. C.; Storhoff, J. J. *Nature (London)* **1996**, *382*, 607. (e) Snow, E. S.; Campell, P. M.; McMarr, P. J. *Nanotechnology* **1996**, *7*, 434. (f) Resch, R.; Baur, C.; Bugacov, A.; Koel, B. E.; Echternach, P. M.; Madhukar, A.; Montoya, N.; Requicha, A. A. G.; Will, P. *J. Phys. Chem. B* **1999**, *103*, 3647. (g) Wilbur, J. L.; Kumar, A.; Biebuyck, H. A.; Kim, E.; Whitesides, G. M. *Nanotechnology* **1997**, *7*, 452. (h) McCarty, G. S.; Weiss, P. S. *Chem. Rev.* **1999**, *99*, 1983, and references therein.
(16) (a) Ulman, A. *An Introduction to Ultrathin Organic Films*; Academic Press: San Diego, 1991. (b) Ulman, A. *Chem. Rev.* **1996**, *96*, 1533.
(17) (a) Nuzzo, R. G.; Allara, D. L. *J. Am. Chem. Soc.* **1983**, *105*, 4481. (b) Schlotter, N.; Porter, M.; Bright, T.; Allara, D. L. *Chem. Phys. Lett.* **1986**, *132*, 93. (c) Maoz, R.; Sagiv, J. *J. Colloid Interface Sci.* **1984**, *100*, 465. (d) Lee, H.; Kepley, L.; Hong, H.; Mallouk, T. *J. Am. Chem. Soc.* **1988**, *110*, 618.
(18) (a) Gupta, S.; Uhlmann, P.; Agrawal, M.; Lesnyak, V.; Gaponik, N.; Simon, F.; Stamm, M.; Eychmüller, A. *J. Mater. Chem.* **2008**, *18*, 214–220. (b) Ionov, L.; Sapra, S.; Synytska, A.; Rogach, A. L.; Stamm, M.; Diez, S. *Adv. Mater.* **2006**, *18*, 1453–1457. (c) Mitsuishi, M.; Koishikawa, Y.; Tanaka, H.; Sato, E.; Mikayama, T.; Matsui, J.; Miyashita, T. *Langmuir* **2007**, *23* (14), 7472–7474. (d) Houbenov, N.; Hermsdorf, N.; Tokarev, I.; Sidorenko, A.; Minko, S.; Stamm, M.; Gehrke, R.; Cunis, S. and Müller-Buschbaum, P. Hasylab annual meeting, 2002, part 1.
(19) Gupta, S.; Uhlmann, P.; Agrawal, M.; Chapuis, S.; Oertel, U.; Stamm, M. *Macromolecules* **2008**, *41* (8), 2874.
(20) Minko, S.; Patil, S.; Datsyuk, V.; Simon, F.; Eichhorn, K. J.; Motornov, M.; Usov, D.; Tokarev, I.; Stamm, M. *Langmuir* **2002**, *18*, 289–296.
(21) Beamson, G.; Briggs, D. High resolution XPS of organic polymers. *The Scienta ESCA 300 Database*; J. Wiley & Sons: Chichester, 1992; ISBN 0-471-93592-1.
(22) Experimentally determined for our spectrometer KRATOS AXIS ULTRA.
(23) Iyer, K. S.; Zdyrko, B.; Malz, H.; Pionteck, J.; Luzinov, I. *Macromolecules* **2003**, *36*, 6519–6526.
(24) Matsui, J.; Akamatsu, K.; Nishiguchi, S.; Miyoshi, D.; Nawafune, H.; Tamaki, K.; Sugimoto, N. *Anal. Chem.* **2004**, *76*, 1310–1315.
(25) Luzinov, I.; Iyer, K. S.; Klep, V.; Zdyrko, B.; Draper, J.; Liu, Y. *Polym. Prepr.* **2003**, *44*, 437.
(26) (a) Grabar, K. C.; Freeman, R. G.; Hommer, M. B.; Natan, M. J. *Anal. Chem.* **1995**, *67*, 735–743. (b) Freeman, R. G.; Grabar, K. C.; Allison, K. J.; Bright, R. M.; Davis, J. A.; Guthrie, A. P.; Hommer, M. B.; Jackson, M. A.; Smith, P. C.; Walter, D. G.; Natan, M. J. *Science* **1995**, *267*, 1629–1632.
(27) Nuzzo, R. G.; Dubois, L. H.; Allara, D. L. *J. Am. Chem. Soc.* **1990**, *112*, 558.
(28) Klos, J.; Pakula, T. *Macromolecules* **2004**, *37*, 8145.
(29) Grabar, K. C.; Brown, K. R.; Keating, C. D.; Stranick, S. J.; Tang, S. L.; Natan, M. J. *Anal. Chem.* **1997**, *69*, 471–477.
(30) (a) Weisbecker, C. S.; Merritt, M. V.; Whitesides, G. M. *Langmuir* **1996**, *12*, 3763–3772. (b) Nath, N.; Chilkoti, A. *J. Am. Chem. Soc.* **2001**, *123*, 8197–8202.
(31) Moulder, J. F.; Stickle, W. F.; Sobol, P. E.; Bomber, K. D. In *Handbook of X-ray Photoelectron Spectroscopy*; Chastian, J., Ed.; Perkin-Elmer Corp.: Waltham, MA, pp 182−183.
(32) Briggs, D. *Characterization of Surfaces*; Pergamon: Oxford, 1989.
(33) Seah, M. P.; Dench, W. A. *Surf. Interface Anal.* **1979**, *1*, 2.
(34) Auroy, P.; Auvray, L. *Macromolecules* **1992**, *25* (16), 4134–4141.

(35) (a) Halperin, A. *J. Phys. (Paris)* **1988**, *49*, 547. (b) Zhulina, E. B.; Borisov, O. V.; Pryamitsyn, V. A.; Birshtein, T. M. *Macromolecules* **1991**, *24*, 140.
(36) Grest, G. S.; Murat, M. *Macromolecules* **1993**, *26*, 3108.
(37) Karim, A.; Satija, S. K.; Douglas, J. F.; Ankner, J. F.; Fetters, L. J. *Phys. Rev. Lett.* **1994**, *73*, 3407.
(38) (a) Nie, Z. H.; Fava, D.; Rubinstein, M.; Kumacheva, E. *J. Am. Chem. Soc.* **2008**, *130*, 3683–3689. (b) Nie, Z.; Fava, D.; Kumacheva, E.; Zou, S.; Walker, G. C.; Rubinstein, M. *Nat. Mater.* **2007**, *6*, 609–614.
(39) (a) Kreibig, U.; Vollmer, M. *Optical Properties of Metal Clusters*; Springer-Verlag: Berlin, 1995. (b) Schmid, G., Ed. *Clusters and Colloids, from Theory to Applications*; VCH: New York, 1994. (c) Alivisatos, A. P. *J. Phys. Chem.* **1996**, *100*, 13226. (d) Fendler, J. H.; Meldrum, F. C. *Adv. Mater.* **1995**, *7*, 607.
(40) (a) Teranishi, T.; Hasegawa, S.; Shimizu, T.; Miyake, M. *Adv. Mater.* **2001**, *13*, 1699–1701. (b) Brust, M.; Walker, M.; Bethell, D.; Schiffrin, D. J.; Whyman, R. *J. Chem. Soc., Chem. Commun.* **1994**, 801.
(41) Auroy, P.; Auvray, L. *Langmuir* **1994**, *10* (1), 225–231.
(42) Brandrup, J., Immergut, E. H., Eds.; *Polymer Handbook*, 2nd ed.; John Wiley & Sons: New York, 1975; Vol. *VII*, p 386.
(43) Nath, N.; Chilkoti, A. *Anal. Chem.* **2002**, *74*, 504–509.
(44) Malynych, S.; Luzinov, I.; Chumanov, G. *J. Phys. Chem. B* **2002**, *106*, 1280–1285.

MA801557U